FIRE AND MATERIALS
Fire Mater. 2005; **29**:351–366
Published online 30 June 2005 in Wiley InterScience (www.interscience.wiley.com). DOI: 10.1002/fam.892

Real fire performance of partition assemblies‡,§

Samuel L. Manzello*,†, Richard G. Gann, Scott R. Kukuck,
Kuldeep Prasad and Walter W. Jones

*Building and Fire Research Laboratory, National Institute of Standards and Technology,
Gaithersburg, MD 20899-8662, U.S.A.*

SUMMARY

A series of real-scale compartment tests was performed to provide information on the phenomenology of partition response and failure, to guide model development. Two partition assemblies of 2.44 m × 2.44 m were exposed to two intense fires from the time of ignition to beyond flashover. The assemblies were constructed using type X gypsum panels. The stud spacing and stud dimensions were fixed for both assemblies. Heat flux gauges provided time histories of the energy incident on the partitions, while thermocouples provided data on the propagation of heat through the partitions and on the progress toward perforation. Visual and infrared cameras were used to image partition behavior during the fire exposure. The results obtained from these experiments are discussed. Published in 2005 by John Wiley & Sons, Ltd.

INTRODUCTION

For nearly a century, the cornerstone of fire safety in buildings has been the ability to confine a fire for a time sufficient to allow successful evacuation of the occupants. To effect this, the partitions in a building (walls, floors, ceilings) are rated based on their resistance to the passage of heat and smoke. In the USA, the standard test method for determining these ratings is ASTM E119 [1], first published in 1918 and updated periodically by ASTM Committee E5, Fire Standards. The similar international standard is ISO 834 [2], which is maintained by ISO TC92 SC2, Fire Containment. Rating requirements are then used in a prescriptive manner, based on the use and location of building elements within a structure. The use of these standards has been successful in reducing the number of fires that have killed people, destroyed structures and, in certain instances, devastated entire cities.

Compartmentation is especially important in tall buildings, because egress of numerous occupants can be a complex and time consuming process. Intact barriers prevent the spread of flame, keep the egress paths available, and increase the safe time in places of refuge. For all

*Correspondence to: S. L. Manzello, Building and Fire Research Laboratory, National Institute of Standards and Technology, Gaithersburg, MD 20899-8662, U.S.A.
†E-mail: samuel.manzello@nist.gov

§Official contribution of the National Institute of Standards and Technology.

Received 1 July 2004
Revised 29 March 2005
Accepted 29 March 2005

Table I. Failure characteristics of a non-combustible partition and hazards due to partition failure.

Hazard	Failure characteristic
Thermal ignition of combustibles beyond current fire compartment	Excessive temperature on reverse side of wall
Spread of fire effluent beyond current fire compartment	Cracks (or openings) through wall
Spread of flames beyond current fire compartment	Opening in wall

these functions, it is necessary to know, in terms of real time, how long the interior partitions in a building will contain flames and smoke.

There are three means by which a failure of a non-combustible partition (e.g. wall) can increase the hazard from a building fire and there are three correlated failure modes of the partition, listed in Table I. One means of obtaining information regarding these failure modes could be through the use of large scale furnace testing, as in ASTM E119 [1] or ISO 834 [2]. Furnace testing allows a large section of the actual partition to be evaluated, which is important since partitions are not normally simple one-dimensional constructs. Unfortunately, it has long been known that current fire resistance ratings obtained in furnaces do not coincide with actual safety times, but rather only provide *relative* guidance [1,2]. Thus, a 2 h rated partition may not contain an actual fire for 2 h, but is likely to contain heat and smoke longer than a 1 h rated partition. Both the absolute values and the differences between ratings depend on the nature of the fire and the composition of the particular partition [3–6].

Modeling the response of the partition and its eventual failure would be time and cost efficient. A model would allow an examination of the partition under a variety of different fire types. This would enable integration of performance criteria with effects of other fire mitigation strategies, such as the use of sprinklers or less flammable furnishings. However, there is a significant up-front cost of developing such a model. Partitions are not normally simple one-dimensional constructs. Furthermore, there is an associated cost of obtaining the necessary thermophysical properties of the components for input to the model as well as understanding and integrating the complex mechanics of cracking and perforation of the partition.

To this end, several investigators have recognized the importance of modeling the response of both wood and steel framed partition assemblies to fire exposure [7–13]. Such models can generally only predict the behavior of the partition up to the point of the insulation criterion, as specified under ASTM E119 [1] and ISO 834 [2]. As mentioned, all failure modes are needed to provide an absolute time for how long a partition can contain flames and smoke.

A course was embarked on to provide a methodology for inclusion in the performance-based design of buildings. The research involves obtaining real-scale experimental data, modeling the behavior of partitions as they are driven to failure by the fire, and developing recommendations for obtaining input parameters from modifications to standard fire resistance tests such as ASTM E119 [1] and ISO 834 [2].

This paper presents the results of a series of real-scale compartment tests performed to provide information on the phenomenology of partition response and failure and also quantitative information to guide the model development. It is important to note that these tests were conducted under actual fire conditions rather than in a furnace. The type of partition assembly considered was non-load bearing walls of gypsum panels attached with screws to steel studs. This type of construction was selected since it is the most common interior construction in tall buildings.

EXPERIMENTAL DESCRIPTION

Two types of non-load bearing walls consisting of gypsum panels attached to steel studs were constructed for fire testing. Figure 1 displays the exposed face construction, which was the same for both assemblies. Differences in construction occurred at the unexposed face. The dimensions of each assembly were 2.44 m × 2.44 m. Steel studs (width: 92 mm, thickness: 20 gauge) were spaced at 609 mm and type X gypsum panels (USG Fire Code Core[§]) with a thickness of 15.9 mm were attached vertically to the studs using type S drywall screws spaced at 305 mm. The joints were taped and spackled prior to fire initiation within the compartment. The partitions were constructed under ASTM guidelines for non-load bearing wall assemblies [14–17].

Figure 2(a,b) displays Assembly One, which consisted of two single (1.22 m × 2.44 m) gypsum panels installed on the exposed face. Assembly One, which is not a common construction, was built to visualize the partition response to the fire load. Figure 3(a–c) displays Assembly Two, which consisted of two single (1.22 m × 2.44 m) gypsum panels installed on the exposed face and one (1.22 m × 2.44 m) gypsum panel installed on the unexposed face. Assembly Two was

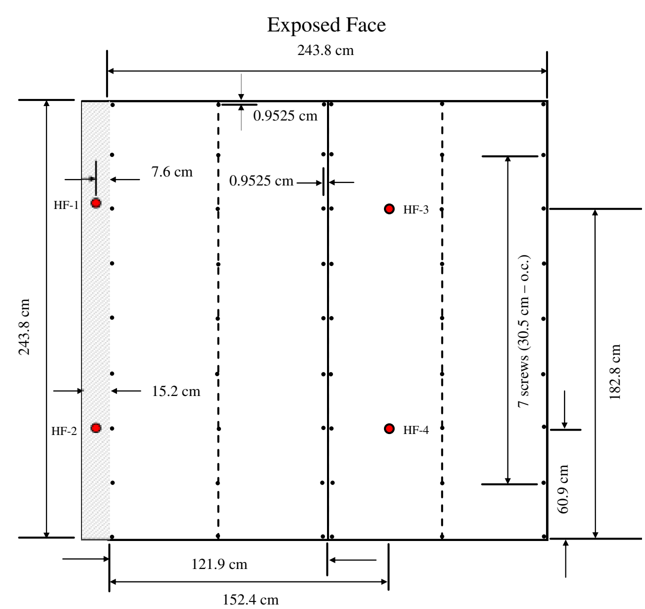

Figure 1. Drawing of partition construction at the exposed face. The location of the total heat flux gauges are shown.

[§]Certain commercial products are identified to describe adequately the experimental procedure. This in no way implies endorsement from NIST.

constructed to investigate the influence of a cavity within the assembly on partition behavior under a fire load. Since only one side of Assembly Two was fitted with a gypsum panel on the unexposed face, it was imperative to seal the service holes in the studs to simulate the cavity that would be created if another gypsum panel was fitted to the left side of the assembly (see Figure 3(a)). To facilitate the explanation of partition behavior observed during the fire exposures, the space between the studs was designated as section 1–section 4 (see Figures 2(a) and 3(a)).

Temperatures were obtained using type K thermocouples (22 gauge) attached to the gypsum panels. Temperatures were measured at: (1) the exposed surface (2) within the gypsum board cavity for the double layer assembly (inside of exposed board, inside of the unexposed board) and (3) on the unexposed face. Bare thermocouples were used both on the exposed face and within the gypsum board cavity. Thermocouples at the unexposed face were placed under insulating pads, as specified in ASTM E119 [1]. This was done in order to compare these

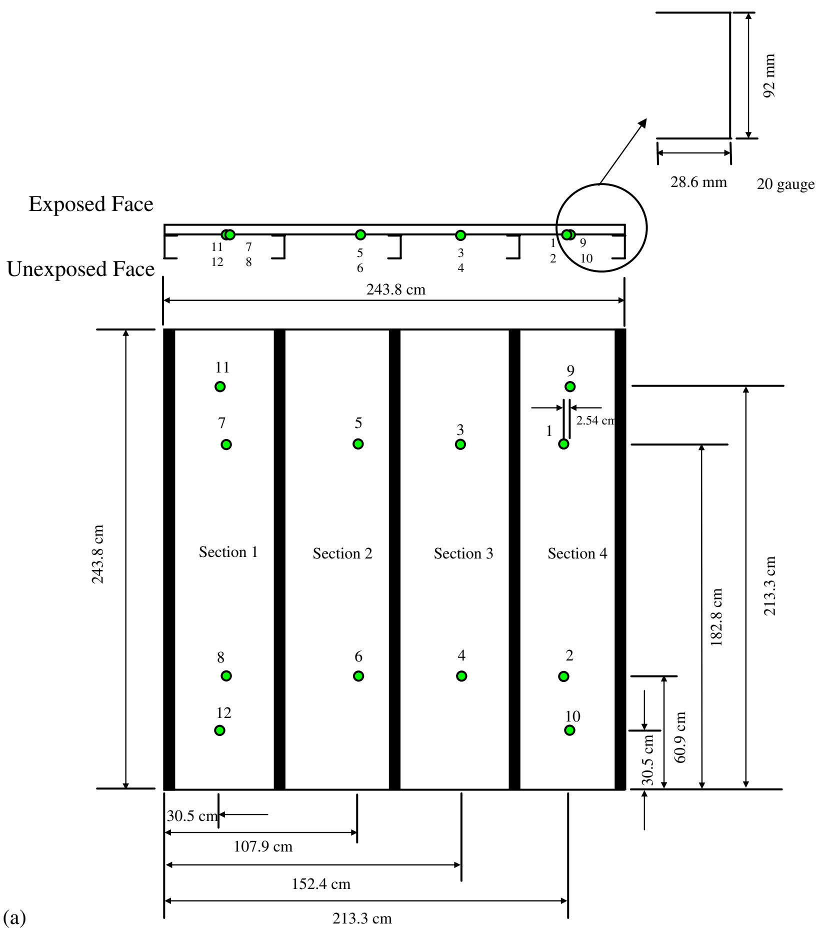

(a)

Figure 2. (a) Drawing of Assembly One showing the location of the unexposed face temperature measurements; and (b) drawing of Assembly One showing the location of the exposed face temperature measurements.

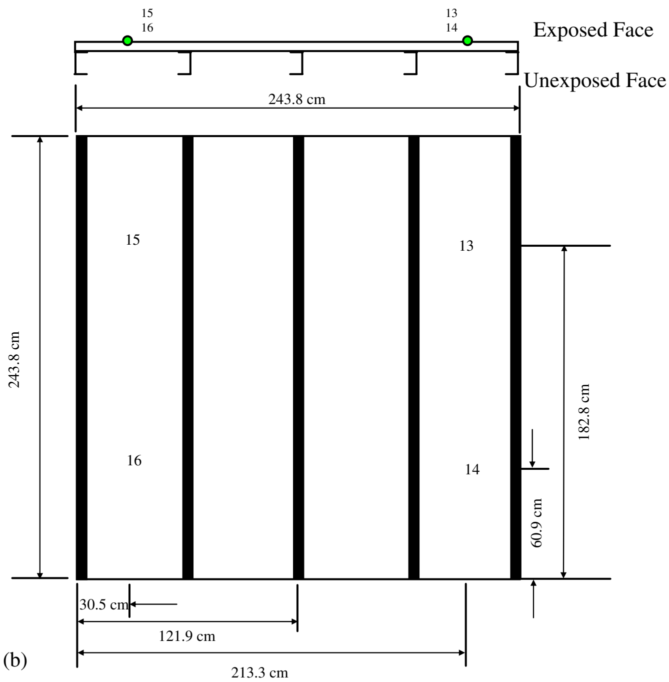

(b)

Figure 2. *Continued.*

measurements with the failure modes of ASTM E119 [1]. To model the unexposed temperatures accurately, one must account for the thermal resistance induced by the pads [10]. The locations of the thermocouples for each assembly are displayed in Figures 2(a,b), 3(a–c).

Four Schmidt-Boelter water cooled total heat flux gauges were used to measure the heat flux incident on the partitions. The position of all four gauges (designated as HF1, HF2, HF3 and HF4) was the same for both partition assemblies tested (see Figure 1). Two gauges were mounted flush to one of the gypsum panels and two gauges were mounted flush to the column adjacent to the other vertically mounted gypsum panel. The gauges were mounted on the column in order to have one of the vertically mounted gypsum panels free from holes necessary for gauge mounting. For the gauges mounted on the gypsum panel, a custom bracket was constructed to support the weight of the gauges and water lines.

To mitigate water condensation on the gauge surface, each gauge was water cooled to 75° C $\pm$ 5° C, which is well above the dew point. Since soot deposition on the gauge surface was not desired, each gauge was purged with nitrogen for 3 s, every 2 min (120 s) during the test. The purge signal was apparent and was removed from the temporal heat flux trace. Each gauge was provided with a calibration from the manufacturer. However, the gauges were re-calibrated at NIST prior to the test series at 75° C. The gauges were subsequently re-calibrated upon completion of the test series. The calibrations before and after the test series agreed to within the uncertainty of the calibration procedure.

The unexposed face of each partition assembly was imaged using a standard (visual) video camera with a framing rate of 30 frames/s. In addition, an infrared camera was used to image the unexposed face, also at 30 frames/s. In order to have the unexposed face fill the field of view of the IR camera, the IR camera had to be placed close to the assembly. Consequently, care was taken to avoid damage to the camera from the heat generated by the fire. This problem was circumvented with the standard video camera by fitting it with an appropriate zoom lens. Both infrared and standard video cameras were recorded on mini-digital video (mini-DV) cassettes for subsequent image analysis. Prior to each test, photographs were taken at 2048 × 1024 pixel resolution of both the exposed and unexposed face using a digital camera fitted with a zoom lens. Another series of photographs were taken of the exposed and unexposed face upon completion of each test.

The size of the compartment for the fire experiments was 10.7 m long × 7.0 m wide × 3.4 m high. A schematic of the compartment is displayed in Figure 3(d). A 2.44 m × 2.44 m opening was constructed on the lower 7.0 m side of the compartment so that each partition assembly could be switched out easily for each fire test. A similar construction and mounting methodology was followed for both assemblies. First, the exposed face was attached to the steel studs. The entire assembly was mounted flush to the ceiling of the compartment and all instrumentation was installed while the partition assembly was mounted. After the first fire was over, Assembly One was removed and Assembly Two was installed.

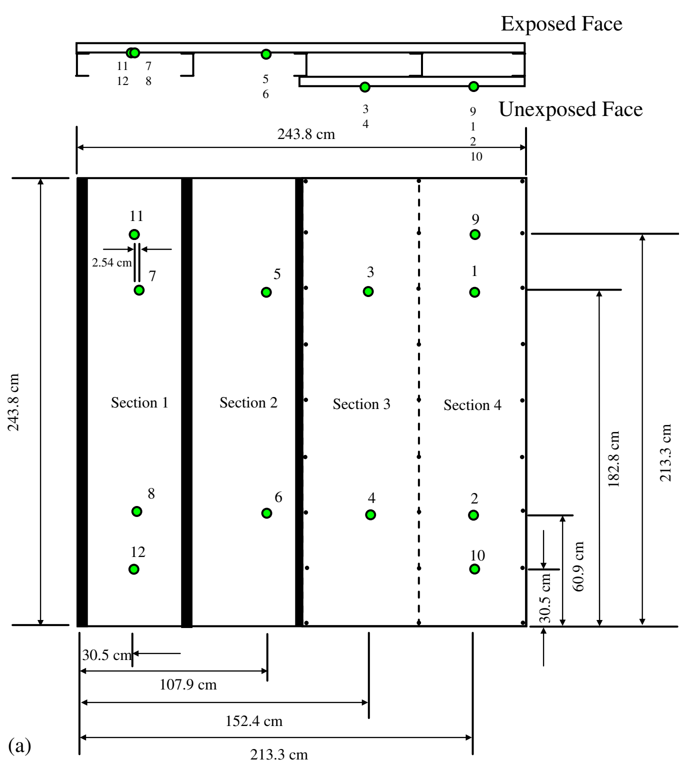

(a)

Figure 3. (a) Drawing of Assembly Two, showing the location of the unexposed face temperature measurements; (b) drawing of Assembly Two, showing the location of the exposed face temperature measurements; (c) drawing of Assembly Two, showing the location of the interior temperature measurements; and (d) schematic of compartment where Assembly One and Assembly Two were installed.

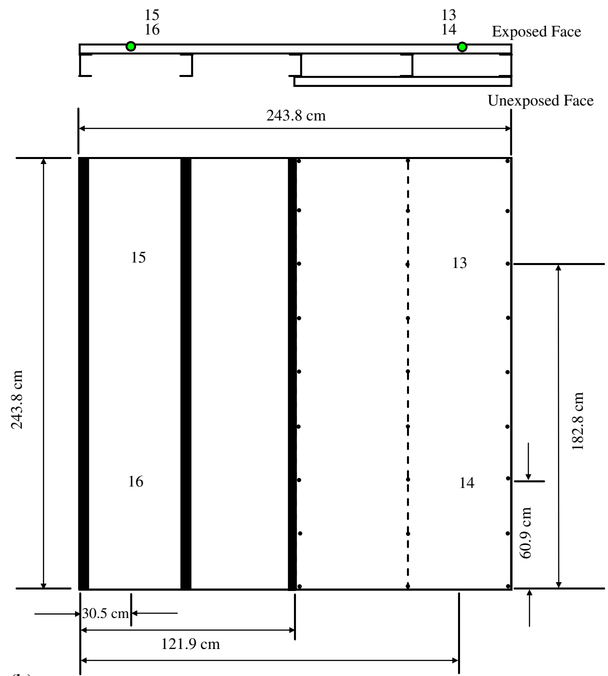

(b)

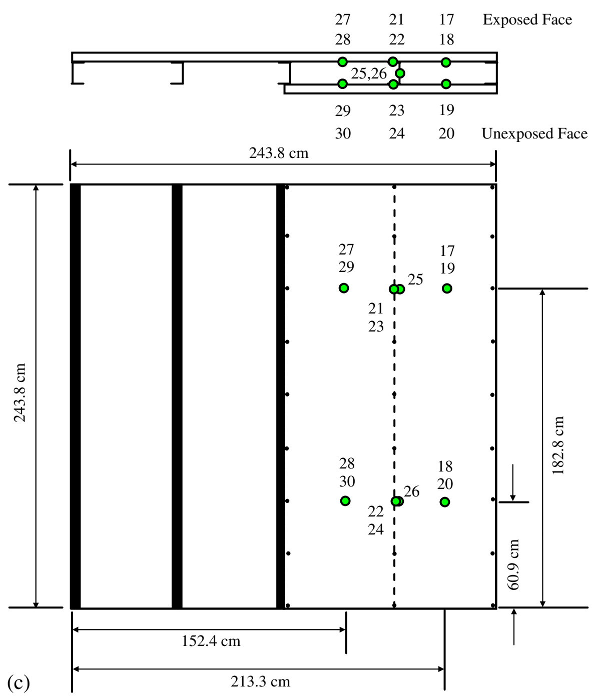

(c)

Figure 3. *Continued.*

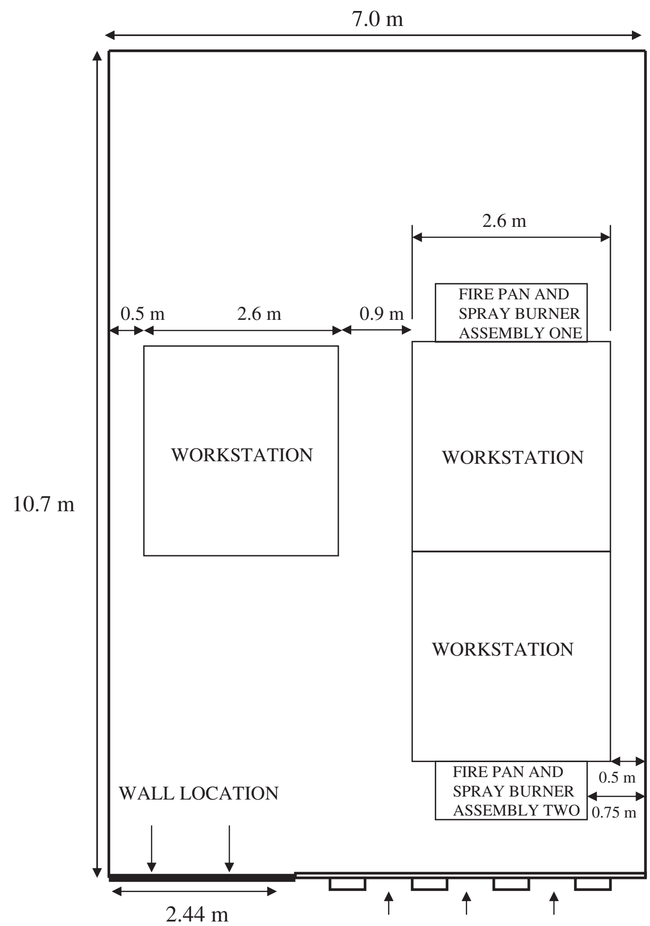

(d)

Figure 3. *Continued.*

The compartment was constructed to simulate a typical office space that would be found in tall buildings. Accordingly, the combustibles within the compartment consisted of three workstations for each of the fire exposures reported here. The fires were ignited using a spray burner (see Figure 3(d)). Assembly One and Assembly Two were exposed to fires with peak heat release rates (HRR) of 13.5 MW and 14.0 MW, respectively. The total burn time for each fire was approximately 45 min. Further details of the compartment and the combustibles within the compartment are available elsewhere [18].

RESULTS AND DISCUSSION

Figure 4(a) displays pictures of Assembly One taken immediately after the fire test. Clearly, the paper on the exposed face burned off and significant cracking occurred on both

(a) (b)

Figure 4. (a) Digital pictures of the exposed face immediately after the fire exposure for Assembly One; and (b) digital pictures of the exposed face immediately after the fire exposure for Assembly Two.

gypsum panels. Upon heating, it is well known that gypsum panels contract due to dehydration [10]. The opening along the seams of the two gypsum panels due to contraction is clearly visible. Cracks were observed to occur at the screw locations. The formation of cracks at the screw locations was expected since it is at these locations that the greatest mechanical stress exists. In addition, a series of transverse cracks were observed to form in both gypsum panels.

While images of the exposed face after the test are useful, it is important to understand how cracks and openings develop within the gypsum panels during the fire exposure. To ascertain this information, the unexposed face was imaged using an infrared (IR) camera and a standard video camera. The temporal evolution of openings and crack propagation was analysed and was observed to occur in the following order: (1) opening at joint between the two vertically mounted gypsum panels ($t = 964\,\mathrm{s}$), (2) cracks at the screw locations along studs ($t = 1306\,\mathrm{s}$) and (3) transverse cracks ($t = 1499\,\mathrm{s}$, crack started in section 2, $t = 1569\,\mathrm{s}$, crack started at section 1). It is important to note that the transverse cracks that formed on the exposed face, corresponding to section 3 and section 4 on the unexposed face, were not visible on the unexposed face.

From these observations, the following conclusion can be inferred about crack and opening formation. It is apparent that at the joint location of the two gypsum panels, the taping compound burned off. Both gypsum panels contracted, resulting in an opening at the joint. The openings were first visible in the upper portion of section 2. Subsequently, the gypsum panels cracked at the screw locations and then transverse cracks appeared. It is imperative to understand the thermal load imparted by the fire to the partition assembly to gain insights into the conditions for crack and opening production.

Plotted in Figure 5(a) are the exposed face temperature measurements collected during the test for Assembly One. It is estimated that combined uncertainty for the temperature measurements are $\pm 10^\circ\,\mathrm{C}$ for temperatures less than $200^\circ\,\mathrm{C}$ and $\pm 30^\circ\,\mathrm{C}$ for temperatures larger

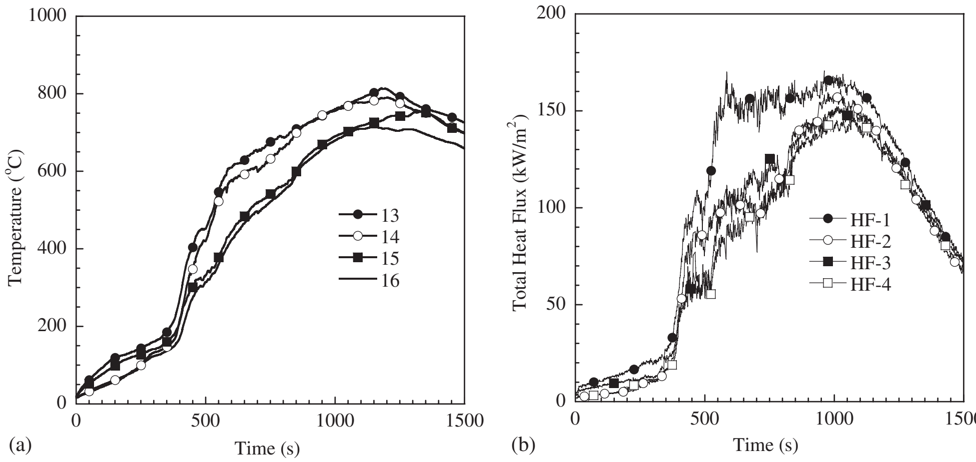

Figure 5. (a) Temporal evolution of the exposed face temperature measurements for Assembly One as a function of location; and (b) temporal evolution of the total heat flux measurements for Assembly One as a function of location.

than 200° C. The temperatures at thermocouple 13 and thermocouple 14 were similar. The same trend was observed for thermocouples 15 and 16. The temperature was the highest at thermocouple locations 13 and 14, as this side of the wall was closer to fire. The rate of the initial temperature rise was also faster at thermocouple locations 13 and 14 as well.

Figure 5(b) displays the temporal evolution of measured total heat flux as function of position within Assembly One. Since soot was not allowed to accumulate on the gauge surface due to the nitrogen purge system, the two main sources of uncertainty in total heat flux measurement were: (1) calibration uncertainty (2) uncertainty associated with the voltage reading process. Uncertainty exists with the calibration itself and the fluctuation of the cooling water temperature during the test, since the calibration was based on a water temperature of 75° C. Accordingly, the relative combined uncertainty in the total heat flux measurements was $\pm 10\%$.

From Figure 5(b), the total heat flux increased most rapidly at location HF-1 and reached a value of $160\,\mathrm{kW/m^2}$ at a time of 550 s after ignition. The total heat flux was highest at locations HF-1 and HF-2. Ultimately, the maximum value of total heat flux occurred at nearly the same time after ignition (1050 s) at all locations and varied from $140\,\mathrm{kW/m^2}$ to $160\,\mathrm{kW/m^2}$.

To understand how the heat propagated through the single 15.9 mm gypsum panel required measurement of the unexposed face temperatures. The unexposed face temperature measurements are reported in Figure 6 for Assembly One. This assembly failed the insulation criterion as specified in ASTM E119 [1] at 1100 s after ignition. For clarity, ASTM E119 [1] specifies that an assembly has failed if the temperature rises more than 180° C at a single-point measurement located under an insulting pad. The temperature rise on the unexposed face was a function of location. Based upon temperature and total heat flux measurements on the exposed face, it is not surprising that temperature rose most quickly at thermocouple locations 1, 3 and 9. It is interesting to note that differences in the magnitude of measured temperatures were also a function of location on the unexposed surface. As these measurements are taken on surfaces not

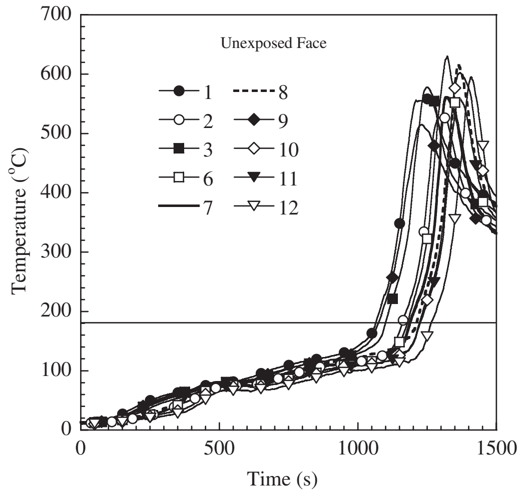

Figure 6. Temporal evolution of the unexposed face temperature measurements for Assembly One as a function of location.

directly exposed to the large heat fluxes of the fire exposure and are taken from underneath a pad, it is estimated that the uncertainty in the measurements is approximately $\pm 10^{\circ}$ C.

From the video-graphic records, the paper on section 4 (far right - see Figure 2(a) of unexposed face) was the first to char. Subsequent to this, the paper began to char on section 3. Section 2 then charred and flaming was observed. The flame originated near the top, and propagated both upward and downward. The flames propagated towards the location of thermocouple 6. After this, flames were visible on the bottom of section 4 (near thermocouple location 10). The last area of extended flaming was observed on section 1. Flames started near thermocouple locations 8 and 12. The flame quickly propagated upwards and engulfed most of section 1 in flames.

The timeline of events from the video-graphic records agreed with the magnitude of the unexposed face temperature measurements. Thermocouple location 6, where the most severe flaming was observed, produced the highest measured temperature. The upper portion of section 1, where the temperature rise was the fastest, produced the lowest temperatures since no flaming was observed at these locations (1,3,9).

Images of the exposed face of Assembly Two are displayed in Figure 4(b). The backside of the gypsum panel on the right (see Figure 4(b)) was open to ambient. The backside of the gypsum panel on the left was enclosed with an outer gypsum panel (see Figure 3(c)). The gypsum panel on the right cracked at the screw locations and a set of transverse cracks formed as a consequence of the fire exposure. These features were qualitatively similar to gypsum panels in Figure 4(a). For the gypsum panel on the left, large gaps occurred at the screw locations. However, transverse cracks did not appear.

Video-graphic records were analysed as a function of time after ignition for Assembly Two. Throughout the test, the unexposed face on the side of the partition with the two gypsum panels did not char or produce open flame. In fact, the unexposed face on this side was visibly unaffected by the fire exposure. As a result, the cracking that resulted inside the panel on this side was not visible in either the IR or standard video view.

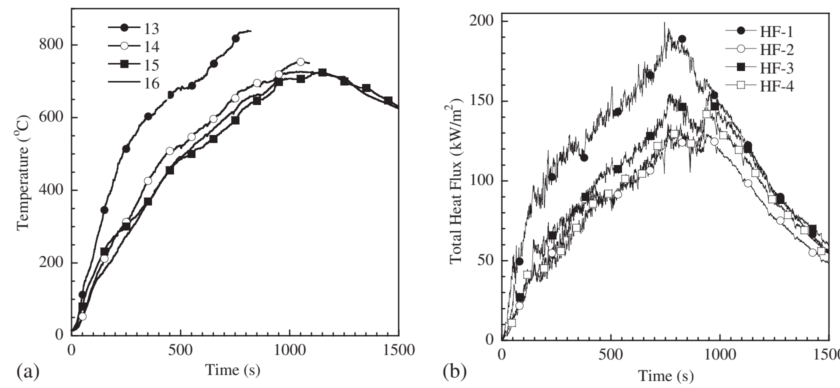

Figure 7. (a) Temporal evolution of the exposed face temperature measurements for Assembly Two as a function of location; and (b) temporal evolution of the total heat flux measurements for Assembly Two as a function of location.

For the single gypsum panel, crack propagation was clearly visible from the video-graphic records. The transverse cracks appeared in section 2 ($t = 1494$ s) and later in section 1 ($t = 1708$ s). It is interesting to note that the order of crack propagation was similar to Assembly One. The openings at the joints between the two vertically mounted gypsum panels and cracks at the screw locations along the studs were not visible in the video records for Assembly Two.

The exposed face temperature measurements for Assembly Two are displayed in Figure 7(a). During this particular test, the thermocouples failed at locations 13 and 14 at 850 s and 1150 s, respectively, into the fire exposure. These failures are speculated to be due to extreme heating of thermocouple connections 13 and 14, which were located inside the gypsum cavity. Complete temperature traces were obtained at thermocouple locations 15 and 16. In spite of the thermocouple failures, enough data were obtained to provide a clear picture of the temperature rise on the exposed surface. From the figure, the largest temperature rise occurred at location 13, followed by thermocouple location 14. Similar to the data obtained for Assembly One, the hotspot within the wall was clearly on the gypsum panel fitted with thermocouples 13 and 14.

Total heat flux data collected during the fire exposure for Assembly Two is displayed in Figure 7(b). At location HF-1, the total heat flux increased rapidly to a peak value of 190 kW/m^2 at a time of 800 s. At this location (HF-1), total heat flux was sustained at more than 150 kW/m^2 for over 500 s. At the other upper position, HF-3, the total heat flux was 30% less than at location HF-1. The total heat flux was similar in magnitude (130 kW/m^2) for the two lower positions, HF-2 and HF-4. Overall, the fire exposure was qualitatively similar to the exposure in which Assembly One was subjected, namely the magnitude of the total heat flux was greatest at locations HF-1 and HF-3.

For partition assemblies constructed with an interior cavity, such as Assembly Two, interior temperature measurements are needed to model the complex heat transfer process that occurs within the cavity [10]. Figure 8(a) displays interior temperature measurements on the inside of the exposed board. Figure 8(b) shows interior temperature measurements on the inside of the unexposed board. In addition, Figure 8(b) shows temperatures obtained within the steel studs (25, 26).

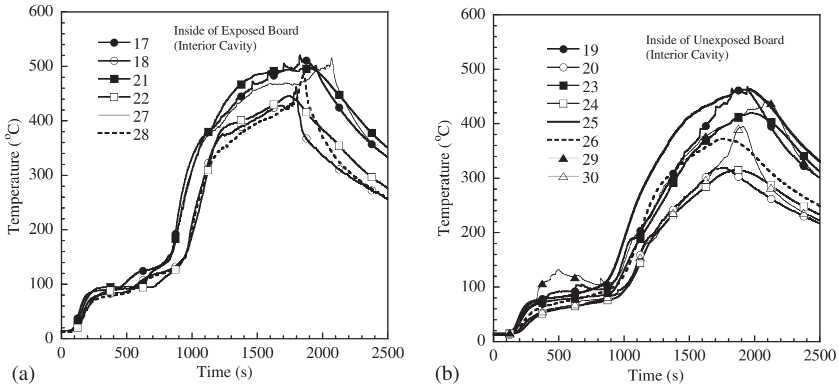

Figure 8. (a) Temporal evolution of temperatures measured on the inside of the exposed face as a function of location; and (b) temporal evolution of temperatures measured on the inside of the unexposed face as a function of location.

Some salient features are apparent from these figures. The temperature rose faster on the inside of the exposed board at all locations compared with those temperatures at the same height on the inside of the unexposed board. For example, a noticeable temperature increase was observed 30 s after ignition (locations 17, 18, 21, 22, 27 and 28). On the contrary, a temperature rise was not detected at locations 19, 20, 23, 24, 29 and 30 until 125 s after ignition. The magnitude of the temperature on the inside of the exposed board was higher than their counterparts on the inside of the unexposed board.

For the temperatures measured on the inside of the unexposed board, the temperatures varied greatly (see Figure 8(b)). For example, at location 19, the measured temperature was 460° C whereas at location 20, the measured temperature was 300° C. As mentioned previously, it was not possible to see into the cavity during the fire test. Accordingly, to understand this difference in measured temperature, this panel was removed after the fire test. Upon inspection of the inside of the unexposed board, the paper was slightly brown near location 20, confirming that the paper did not burn at this location, which explained the lower temperature.

The outside face temperatures of the unexposed board were measured for Assembly Two and are displayed in Figure 9. From the data it is apparent that the temperature rise on the outside face of the unexposed board was minimal. In fact, the temperature rise was insufficient to result in failure under the insulation criterion of ASTM E119 [1]. For the side with the single layer, the temperature rise was significant. The insulation failure criterion [1] was reached at 900 s after ignition. Based upon the total heat flux and exposed face temperature measurements, it is not surprising that the temperature at location 5 rose the quickest. Similar to Assembly One, differences in the maximum temperatures measured on the unexposed surface were observed.

From the video-graphic records of Assembly Two, the paper on section 2 (see Figure 3(a) of unexposed face) was the first to char. Subsequent to this, the paper began to char on section 1. After charring started on section 1, the upper half of panel two began to flame, near thermocouple location 5. The flames spread downwards towards thermocouple location 6. After this, flames were visible on the top of section 1 (near thermocouple locations 7 and 11).

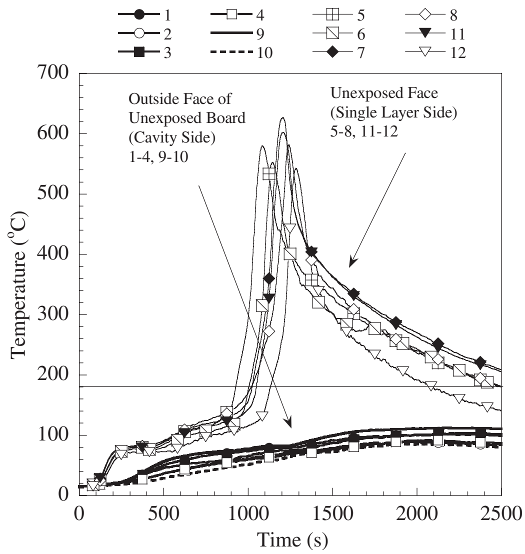

Figure 9. Temporal evolution of the unexposed face temperature measurements for Assembly Two as a function of location.

Similar to Assembly One, the timeline of events from the video-graphic records agreed with the magnitude of the unexposed face temperature measurements. Locations where the most severe flaming was observed (5, 7 and 11) produced the highest measured temperature. The lower portion of section 1, near thermocouple location 12, produced the lowest temperatures since flaming was not observed at this location.

It is crucial to compare the measurements obtained for Assembly One and Assembly Two with data in the open literature. To the author's knowledge, no data exist in the open literature for partition assembly behavior under actual fire conditions. Rather, most data that are available for partition assemblies have been obtained in test furnaces. Accordingly, the total heat flux measured under the real fire exposures was compared with those obtained in large scale furnaces. Sultan *et al.* [19] have performed heat flux measurements in a large-scale furnace designed to test walls and floors. In these experiments, two total heat flux gauges were mounted into a partition assembly and the assembly was subjected to the furnace exposure. Based on their findings, the total heat flux measured was nearly identical (within 2%) at the two gauge locations. The total heat flux reached a value of 150 $\mathrm{kW/m^2}$ in 100 min (6000 s). The furnace was operated up to 120 min (7200 s), where a maximum total heat flux of 170 $\mathrm{kW/m^2}$ was measured.

Comparing these results to Figures 5(b) and 7(b), differences are observed under the present fire conditions. For fires reported here, the total heat flux was clearly a function of height. In addition, the rate of increase of total heat flux measured in the furnace was slower than measurements in the present fire environments. For example, in Figure 7(b), the total heat flux reached 100 $\mathrm{kW/m^2}$ in 700 s. In the furnace, this did not occur until 40 min (2400 s). This suggests that the amount of energy incident on the partition occurs more quickly in these specific fire tests. Experiments with very different room fires by Fang [20] also showed this faster rise.

To the author's knowledge, temperature data for partitions such as Assembly One are not available in the open literature since this is not a common construction. Furnace test data are available for partitions similar to Assembly Two. Sultan [10] performed large-scale furnace tests for non-load bearing steel stud wall assemblies with similar stud spacing (600 mm) and stud width (92 mm) as the present assemblies. The overall size was slightly larger than the assemblies reported here (3.05 m $\times$ 3.66 m). Sultan [10] performed thermocouple measurements inside the cavity at similar locations to Assembly Two. In addition, unexposed face temperature measurements under insulating pads were also reported.

Sultan [10] reported average temperatures at various locations and ran the test up to the time of insulation failure [1], which occurred at 65 min (3900 s). The difference between the measurements of Sultan [10] and those of Assembly Two are the rate of temperature rise, both inside the cavity and on the outside face of unexposed board. Although Assembly Two did not reach insulation failure, the rate of temperature rise both inside the cavity and on the outside face of unexposed board was faster than the assembly subjected to the furnace test. Based on the specific fire exposure data reported here, the heating process inside the furnace can be slower than actual fire conditions.

CONCLUSIONS

Two partition assemblies of 2.44 m $\times$ 2.44 m were exposed to two intense fires from the time of ignition to beyond flashover. During the fire exposure, temperatures were measured at the exposed surface, within the gypsum board cavity for the double layer assembly, and at the unexposed face. Heat flux gauges were used to measure the time histories of the energy incident on the partitions and visual and infrared cameras were used to image the unexposed face during fire testing.

For Assembly One, it was observed that opening and crack propagation ensued in the following order: (1) opening at joint between the two vertically mounted gypsum panels, (2) cracks at the screw locations along studs, (3) transverse cracks in panel 1 and panel 2. Data collected for the partition Assembly Two were compared with data for similar partition assemblies within the literature. Based on these comparisons, the rate of temperature rise both inside the cavity and on the outside face of the unexposed board was faster under these specific fires than a similar assembly subjected to a furnace exposure. In these fires, as opposed to a furnace, the total heat flux was clearly a function of height. In addition, the rate of increase of total heat flux measured in the furnace was slower than the measurements in these specific fire environments.

The detailed photographic measurements, in concert with heat flux and temperature measurements, have generated data for structural failure models. A complementary modeling effort [21] is using the collected data for model validation.

ACKNOWLEDGEMENTS

The authors are indebted to the staff of the Large Fire Laboratory (LFL) at NIST for assistance in the experiments. In particular, we are grateful to Mr Alexander Maranghides, Mr Jay McElroy, Mr Lauren DeLauter, Mr Ed Hnetovsky, Mr Gale Miller and Mr Marco Fernandez. Mr Alex Maranghides provided details necessary for Figure 3(d). Dr Thomas Ohlemiller of BRFL-NIST is acknowledged for his guidance in performing total heat flux measurements. In addition, Dr Ohlemiller designed the nitrogen purge system for the gauges.

REFERENCES

1. *Test Method for Fire Resistance Tests of Building Construction and Materials*. ASTM E119-00a. American Society for Testing and Materials: West Conshohocken, PA.
2. *Fire Resistance Tests – Elements of Building Construction*. ISO 834 Parts 1–9. International Organization for Standardization: Geneva, Switzerland.
3. Bukowski RW. Prediction of the structural fire performance of buildings. *8th Fire and Materials Conference*, *San Francisco*, *CA*, *2003*. InterScience Communications Limited: London, UK.
4. Keltner NR, Moya JL. Defining the thermal environment in fire tests. *Fire and Materials* 1989; **14**:133–138.
5. Grosshandler WL. (ed.). *Fire Resistance Determination and Performance Prediction Research Needs Workshop*: *Proceedings*, *NISTIR 6890*, 2002. NIST: Gaithersburg, MD, USA.
6. CIB-W14. *Rational Fire Safety Engineering Approach to Fire Resistance of Buildings*. Publication 269 (2001).
7. Takeda H. A model to predict the fire resistance of non-load bearing wood-stud walls. *Fire and Materials* 2003; **27**:19–39.
8. Takeda H, Mehaffey JR. Wall2D: A model for predicting heat transfer through wood-stud walls exposed to fire. *Fire and Materials* 1998; **22**:133–140.
9. Richardson LR, Batista M. Revisiting the component additive method for light-frame walls protected by gypsum board. *Fire and Materials* 1997; **21**:107–114.
10. Sultan MA. A model for predicting heat transfer through noninsulated unloaded steel-stud gypsum board wall assemblies exposed to fire. *Fire Technology* 1996; **32**:239–259.
11. Axenenko O, Thorpe G. The modeling of dehydration and stress analysis of gypsum plasterboards exposed to fire. *Computational Materials Science* 1996; **6**:281–294.
12. Mehaffey JR, Cuerrier P, Carisse G. A model for predicting heat transfer through gypsum-board/wood-stud walls exposed to fire. *Fire and Materials* 1994; **18**:297–305.
13. Fredlund B. Modeling of heat transfer and mass transfer in wood structures during fire. *Fire Safety Journal* 1993; **20**:39.
14. *Standard Specification for Installation of Steel Framing Members to Receive Screw-Attaced Gypsum Panel Products*. ASTM C754-00. American Society for Testing and Materials: West Conshohocken, PA.
15. *Standard Specification for Application of Finishing of Gypsum Board*. ASTM C840-03. American Society for Testing and Materials: West Conshohocken, PA.
16. *Standard Specification for Nonstructural Steel Framing Members*. ASTM C645-00. American Society for Testing and Materials: West Conshohocken, PA.
17. *Standard Specification for Steel-Piercing Tapping Screws for the Application of Gypsum Panel Products or Metal Plaster Bases to Wood or Steel Studs*. ASTM C1002-01. American Society for Testing and Materials: West Conshohocken, PA.
18. Hamins A, Maranghides A, McGrattan K, Ohlemiller T, Anleitner R. *Federal Building and Fire Safety Investigation of the World Trade Center Disaster*: *Experiments and Modeling of the Multiple Workstations Burning in a Compartment*. *NIST NCSTAR 1-5E*, 2005. NIST: Gaithersburg, MD, USA.
19. Sultan MA, Benichou N, Min BY. Heat exposure in fire resistance furnaces: full-scale vs intermediate-scale. *8th Fire and Materials Conference*, *San Francisco*, *CA*, *2003*. InterScience Communications Limited: London, UK.
20. Fang JP. *Fire Development in Residential Basement Rooms*. *NBSIR 80-2120*, 1980. InterScience Communications Limited: London, UK. NIST: Gaithersburg, MD, USA.
21. Kukuck S, Prasad K. Heat and mass transfer through gypsum partitions subjected to fire exposure. *Structures in Fire Meeting*, *Ottawa*, *2004*. NRC: Ottawa, Canada.